

A novel *ex vivo* experimental setup to investigate how food components stimulate the enteroendocrine secretions of different intestinal segments

Iris Ginés, Katherine Gil-Cardoso, Paula Robles, Luis Arola,
Ximena Terra, Mayte Blay, Anna Ardévol, and Montserrat Pinent

J. Agric. Food Chem., **Just Accepted Manuscript** • DOI: 10.1021/acs.jafc.8b03046 • Publication Date (Web): 27 Aug 2018

Just Accepted

“Just Accepted” manuscripts have been peer-reviewed and accepted for publication. They are posted online prior to technical editing, formatting for publication and author proofing. The American Chemical Society provides “Just Accepted” as a service to the research community to expedite the dissemination of scientific material as soon as possible after acceptance. “Just Accepted” manuscripts appear in full in PDF format accompanied by an HTML abstract. “Just Accepted” manuscripts have been fully peer reviewed, but should not be considered the official version of record. They are citable by the Digital Object Identifier (DOI®). “Just Accepted” is an optional service offered to authors. Therefore, the “Just Accepted” Web site may not include all articles that will be published in the journal. After a manuscript is technically edited and formatted, it will be removed from the “Just Accepted” Web site and published as an ASAP article. Note that technical editing may introduce minor changes to the manuscript text and/or graphics which could affect content, and all legal disclaimers and ethical guidelines that apply to the journal pertain. ACS cannot be held responsible for errors or consequences arising from the use of information contained in these “Just Accepted” manuscripts.

1 **A novel *ex vivo* experimental setup to assay the vectorial transepithelial**
2 **enteroendocrine secretions of different intestinal segments**

3 Ginés, Iris;¹ Gil-Cardoso, Katherine;¹ Robles, Paula;¹ Arola, Luis;² Terra, Ximena;¹
4 Blay, Mayte;¹ Ardévol, Anna;¹ Pinent Montserrat¹

5 ¹MoBioFood Research Group. ²Nutrigenomics Research Group. Departament de
6 Bioquímica i Biotecnologia, Universitat Rovira i Virgili, Tarragona (Spain).

7

8

9 Corresponding author: Anna Ardévol, Departament de Bioquímica i Biotecnologia,
10 Universitat Rovira i Virgili, c/ Marcel·lí Domingo, nº1, 43007, Tarragona, Spain. Phone:
11 34 977 55 9566, Email: anna.ardevol@urv.cat

12

13

14

15 **Abstract**

16 The enteroendocrine system coordinates gastrointestinal (GI) tract functionality and the whole
17 organism. However, the scarcity of enteroendocrine cells and their scattered distribution make
18 them difficult to study. Here, we glued segments of the GI wall of pigs to a silicon tube,
19 keeping the apical and the basolateral sides separate. The fact that there was less than 1% of
20 70-kDa fluorescein isothiocyanate (FITC)-dextran on the basolateral side proved that the gluing
21 was efficient. Since the lactate dehydrogenase leakage at basolateral side was lower than 0.1%
22 (1.40 ± 0.17 nKatal) it proved that the tissue was viable. The intestinal barrier function was
23 maintained as it is in segments mounted in Ussing chambers (the amount of Lucifer Yellow
24 crossing it, was similar between them; respectively % LY: 0.48 ± 0.13 ; 0.52 ± 0.09 ; $p > 0.05$).
25 Finally, apical treatments with two different extract produced differential basolateral
26 enterohormone secretions (basolateral PYY secretion vs control; animal extract: 0.35 ± 0.16 ;
27 plant extract: 2.5 ± 0.74 ; $p < 0.05$). In conclusion, we report an *ex vivo* system called “Ap-to-Bas”
28 for assaying vectorial transepithelial processes that makes it possible to work with several
29 samples at the same time. It is an optimal device for enterohormone studies in the intestine.

30 **Keywords:** enteroendocrine system, gut hormone secretion, *ex vivo* model,
31 transepithelial activity, food bioactives.

32

33

34

35 **Introduction**

36 As sources of energy and the building blocks of essential constituents, food
37 components play a key role in building and renewing the body. Also, through chemical
38 and mechanical signalling in the gastrointestinal (GI) tract, they provide essential
39 information for the homeostasis of the whole body. The enteroendocrine system is one
40 of the largest endocrine organs in the body. It collects information at the entrance of the
41 organism about what is being taken in and secretes signalling molecules in response.
42 This information is sent to central control systems and used to coordinate homeostatic
43 systems (for example, body energetics). The role, function and mechanisms of the
44 enteroendocrine system are only partially understood [1], [2]. One of the reasons for
45 this lack of understanding is its distribution: it is the sum of lots of cells scattered
46 throughout the intestine, with a low abundance of each type of enteroendocrine cell[3].

47 The most physiological and integrative approach to studying the enteroendocrine
48 system works with the whole animal. Some authors administer the substances to be
49 tested to specific areas of the GI and then obtain samples of blood from specific
50 draining blood vessels and/or cut nerve communication with the central nervous
51 system [4],[5]. This approach requires a huge number of animals, which is
52 problematical from an ethical point of view, and researchers who are highly skilled in
53 surgical procedures. A different approach is to work in vitro with enteroendocrine cell
54 lines. These are useful for highly controlled mechanistic studies, but the physiological
55 response is sometimes quite different from the in vivo response. The most common
56 enteroendocrine cell lines are STC-1 [6] and Glutag [7], which mimic L-cells.
57 Additionally, ghrelin can be studied with attached MNG-3 (derived from mice gastric
58 ghrelinoma [8]) and the unattached (SG-1 or PG-1[9]) cell lines. One of the reasons for
59 the different responses from animals and cell lines may be the lack of vector flux in the
60 treatments. Most studies were carried out in cells attached to the surface in a 2D
61 situation, quite different from the polarised epithelial position in vivo. To overcome

62 these culture limitations, 3D strategies such as gut-on-a-chip [10] have evolved to
63 mimic intestinal fragments, although there are no reports on how effective they are in
64 enteroendocrine studies.

65 Ex-vivo approaches, such as everted sacs, perfused intestinal loops, Ussing chambers,
66 intestinal punches, precision-cut intestinal slices (PCIS) and organoids [11], are in
67 between the previous options, as they use natural intact tissue structures in different
68 controlled approaches [12]. Ussing chambers are widely used to address the need for
69 vectorial processes [13], [14]. They locate the mucosal epithelium in an apical to
70 basolateral position in a hermetic situation with concomitant control of barrier
71 properties. The main drawback is that it is difficult to have enough samples to minimise
72 variability, largely because each device only has a few chambers and is also usually
73 very expensive [15] [16] [17]. To overcome these limitations some authors work with *ex*
74 *vivo* tissue fragments from animal intestines [18][19]. These crude explants from
75 animal intestines make it possible to produce numerous replicates, depending on the
76 animal's size. Although the treatment reaches all the exposed areas of the tissue, it
77 does not mimic the effect of the apical stimulation that takes place in the *in vivo*
78 gastrointestinal tract.

79 We have developed a setup called Ap-to-Bas (AtB). It is an *ex vivo* system that
80 combines the tissue that is readily available in the intestine of pigs, an animal with a
81 metabolism that is similar to that of a human being [20], together with the vectoriality
82 provided by a system that mimics a Ussing chambers approach. Our setup could be a
83 useful tool to screen agents that modulate enteroendocrine secretions throughout the
84 apical and/or basolateral epithelial intestinal areas.

85

86 **Materials & Methods**

87

88 Chemicals

89 Most of the chemicals used – formaldehyde, ethanol, xylol, dimethyl benzene, paraffin,
90 D-mannitol, D-glucose, HEPES, CaCl₂, MgCl₂, KCl, NaCl, NaHCO₃, NaH₂PO₄, 70-kDa
91 fluorescein isothiocyanate (FITC)-dextran, IBMX (I7018) – were purchased from
92 Sigma-Aldrich (Madrid, Spain).. The tissue adhesive used on the animals was 3M
93 Vetbond (Cat 1469SB, St. Paul, USA). Lucifer Yellow (LY-452 Da) was from BTIU
94 80016, Merck, (Darmstadt, Germany). The lactate dehydrogenase (LDH) kit was
95 obtained from QCA (Amposta, Spain).
96 The ELISA kits for total GLP-1 (GLP1-T) (Cat. # EZGLPT1-36k), active GLP-1 (GLP1-
97 A) (Cat. # EGLP-35K) and acyl-ghrelin (cat. # EZRGRA-90K) were purchased from
98 Millipore (Billerica, MA, USA). We obtained Elisa kits for CCK (Cat. No: EKE-069-04)
99 and PYY (Cat. No: FEK-059-03) from Phoenix Pharmaceuticals (Burlingame, CA,
100 USA).

101

102 Collection of the tissue

103 Intestinal tissues were obtained from female pigs (*Sus scrofa domesticus*, *LANDRACE*
104 *X LARGEWHITE*) that were killed for meat production at a local slaughterhouse. Forty-
105 eight pigs were used in the study, all from the same farm. For each assay the number
106 of replicates has been indicated as “n”. Pigs were commercial breeds (18% protein;
107 5.7% lipid; 4.9% fibre; 6.7% ashes; 1.03% Lys; 0.3% Met; 0.78% Calcium; 0.73
108 Phosphorus; 0.20% sodium, Coperal, Santa Coloma de Queralt, Spain) that weighed
109 approximately 120 kg at slaughter and had been fasted for approximately 24 h prior to
110 slaughter. Just 5 min after slaughter, the intestines were excised, and segments of
111 various anatomical regions were stored in ice-cold oxygenated (95% O₂,5%CO₂) KRB
112 buffer (Hepes 11.5 mM, CaCl₂ 2.6 mM, MgCl₂ 1.2 mM, KCl 5.5 mM, NaCl 138 mM,
113 NaHCO₃ 4.2 mM, NaH₂PO₄ 1.2 mM) (Sigma-Aldarich, Madrid, Spain) with D-Manitol 10

114 mM (Sigma-Aldarich, Madrid, Spain). Duodenum (10 cm of intestine taken from the
115 pylorus), distal ileum (10 cm of intestine taken from the ileocaecal junction) and
116 proximal colon (10 cm of intestine taken downstream of the ileocaecal junction) were
117 collected for the experiments.

118 Tissues were transported in KRB buffer to the laboratory at 4 °C and immediately used
119 for *ex vivo* experiments. The time between excision and the beginning of the
120 experiments was approximately 30 min.

121 In the laboratory, the intestine was rinsed with cold KRB buffer (with D-Manitol 10 mM)
122 and mounted in a plastic tube to facilitate the removal of the outer muscle layers. Then,
123 the intestinal tube was cut open longitudinally, and the mucosal tissue was placed
124 apical side up. Circles of tissue with a diameter of 14 mm (approximately 1.54 cm²)
125 were punched out using a biopsy punch (Figure 1a). Twelve circles were taken from
126 each segment from each animal. The intestinal segments were randomized, per region,
127 in a beaker glass. The entire process took around 20 minutes, and the whole time the
128 sample was kept at a low temperature with cold buffer and an ice-cold bath.

129

130 **Building the Ap-to-Bas (AtB) system**

131 We cut a silicon tube with an internal diameter of 8 mm and an external diameter of 12
132 mm into pieces 1.5 cm long with a perfectly flat surface. Tissue adhesive for animal use
133 (3M Vetbond, Cat 1469SB, St. Paul, USA) was lightly applied to the flat side of the
134 tube, which was then gently pressed onto the apical side of the intestinal segment [21].
135 After 10 seconds, the intestine was placed inside a cell culture insert with no bottom
136 membrane (Cat MCRP12H48, 12-well hanging inserts) (Figure 1b). The entire insert
137 containing the tissue segment and the piece of tube was placed in one of the wells of a
138 12-well plate prefilled with 1 ml of KRB buffer (with D-Glucose 10 mM). Apically, the
139 tube was filled with 400 µl of KRB buffer (with D-Mannitol 10 mM). The tissues were

140 then pre-incubated at 37 °C for 15 min in a humidified incubator (5% (v/v) CO₂) (Figure
141 1c).

142 A 70-kDa fluorescein isothiocyanate (FITC)-dextran was used (Sigma Aldrich, St.
143 Louis, MO, USA) to assess the efficiency of the gluing process. FITC-70 kDa was
144 added apically (0.10 mg/mL), and after 60 minutes of incubation, the apical and the
145 basolateral media were collected, centrifuged to precipitate the debris and stored at -20
146 °C for further analysis. The amount of fluorescent dye that crossed to the basolateral
147 side was measured using a Perkin-Elmer LS- 30 fluorimeter (Beaconsfield, UK) at λ_{exc}
148 430 nm; λ_{em} 540 nm.

149

150 **Ussing chamber methodology**

151 Intestinal segments of 0.5 cm² were mounted in Ussing chambers apparatus (DIPL.-
152 ING. K. MUSSLER-SCIENTIFIC INSTRUMENTS, Aachen, Germany). Up to 6
153 segments from each animal were used. Mucosal compartments were filled with 1.5 ml
154 KRB buffer (with D-Mannitol 10 mM) and the serosal compartments were filled with
155 KRB buffer (with D-Glucose 10 mM) [14]. The chambers were kept at 37 °C and
156 continuously oxygenated, 95% O₂ /5% CO₂, with a circular gas flow. Before the
157 experiments were started, the tissues were equilibrated for 15 min in the chambers to
158 achieve steady-state conditions in transepithelial potential differences.

159 The transmucosal potential difference was continuously monitored under open circuit
160 conditions and recorded using 0.8 mm Ag/AgCl Glas-Electrodes. Ohm's law was used
161 to calculate the basal transepithelial electrical resistance (TEER) from the voltage
162 deflections induced by bipolar constant current pulses of 50 mA (every 60 s) with a
163 duration of 200 ms and applied through platinum wires (Mussler Scientific Instruments,
164 Aachen, Germany).

165 After the 20-minute equilibration period, the mucosal side of the biopsies was subject to
166 treatment.

167 **Paracellular transport (Lucifer Yellow assay)**

168 To evaluate the integrity of the intestinal barrier in AtB and Ussing chambers, a solution
169 of Lucifer Yellow (LY-452 Da, BTIU 80016, Merck, Darmstadt, Germany) was used
170 [22]. In this study, 0.4 ml of LY 100 μ M was added to the apical side and after 30, 60
171 and/or 90 minutes of treatment, the apical and the basolateral media were collected,
172 centrifuged to precipitate the debris and stored at -20 °C for further analysis. The
173 amount of fluorescent dye that crossed to the basolateral side was measured using a
174 Perkin-Elmer LS-30 fluorimeter (Beaconsfield, UK) at λ_{exc} 430 nm; λ_{em} 540 nm.

175 **Viability test**

176 Tissue viability was checked by measuring Lactate Dehydrogenase (LDH) with an LDH
177 kit (QCA, Amposta, Spain). Tissues were homogenized in ice-cold KRB buffer with a
178 Tissue Lyser (Qiagen, Hilden, Germany) for 2 min at 50 oscillations/0.5 seg. After
179 centrifugation, supernatant LDH was measured. Cell culture was centrifuged to
180 eliminate debris, and the supernatant was used for the LDH Assay. The amount of LDH
181 activity found in the culture media was considered to indicate the health of the tissue
182 sample throughout the incubation period. The percentage of LDH leakage vs total LDH
183 was used as a viability test [23][16].

184

185 **Study of the enteroendocrine function**

186 To test the enteroendocrine function, we measured the basolateral presence of
187 enterohormes in basal (unstimulated) or apically stimulated conditions. IBMX (I7018,
188 Sigma-Aldarich, Madrid, Spain) 20 μ mol/L was used as positive control [24], and
189 natural extracts of animal and plant origin were used to test the differential ability to

190 stimulate enterohormone secretion in the AtB system. Animal protein homogenate was
191 obtained from pork meat and diluted to 10 mg protein/mL in KRB with D-glucose and
192 protease inhibitors. Vegetal Grape Seed Proanthocyanidin extract (GSPE) was diluted
193 to 100 mg/mL in the same buffer. Treatments were initiated by replacing the apical
194 KRB buffer solution with 400 μ L of pre-warmed KRB buffer (37 °C) [24] containing the
195 test compounds. KRB buffer with D-glucose was used as a control. After 30 minutes of
196 the treatment an aliquot of 200 μ L was picked from the basolateral side of the AP-to-
197 Bas system. Finally, 60 minutes (for ileum and colon) or 90 minutes (for duodenum)
198 after the beginning of the experiment, the whole of the apical and basolateral sides was
199 frozen and stored at -80 °C for further analysis of total and active GLP-1, PYY, CCK
200 and acyl-ghrelin.

201 The enterohormones were assayed using commercial ELISA kits for total GLP-1
202 (GLP1-T) (Cat. # EZGLPT1-36k), active GLP-1 (GLP1-A) (Cat. # EGLP-35K), acyl-
203 ghrelin (cat. # EZRGRA-90K) (Millipore, Billerica, MA, USA), CCK (Cat. No: EKE-069-
204 04) and PYY (Cat. No: FEK-059-03) (Phoenix Pharmaceuticals, Burlingame, CA, USA)
205 following the manufacturer's instructions.

206 **Histology**

207 Intestinal segments of the duodenum, ileum and colon samples were fixed in 4%
208 diluted formaldehyde. After 24 hours of fixation, successive dehydration
209 (Alcohol/Ethanol 70%, 96% and 100%; plus xylol/Dimethyl benzene) and paraffin
210 infiltration-immersion took place at 52°C (Citadel 2000. Thermo Scientific). Then,
211 sections 2 μ m thick (Microm HM 355S. Thermo Scientific) were obtained, deposited on
212 slides (JP Selecta Paraffin Bath) and subjected to automated haematoxylin-eosin
213 staining (Varistain Gemini. Shandom. Thermo) [25].

214

215 **Statistical analysis**

216 Results were expressed as the mean \pm standard error of the mean (SEM). Student's T-
217 test was used to compare the treatments with the control. The one-way ANOVA test
218 was used for multiple comparisons. P-values < 0.05 were considered to be statistically
219 significant. The calculations were performed using XL-Stat 2017 software.

220

221

222

223 **Results**

224 Structure, viability and barrier properties of the intestinal fragments in the AtB

225 Our setup, called Ap-to-Bas (AtB), enables vectorial transepithelial processes prepared
226 from different areas of the intestinal tract *ex vivo* to be assayed. As **Figure 2** shows,
227 the intestinal mucosa and submucosa were easily separated from the muscularis.

228 The viability of the mucosa and submucosa was checked by measuring the amount of
229 lactate dehydrogenase released to the basolateral side of the AtB setup. **Table 1**
230 shows the amount of LDH activity of two representative segments (ileum and colon). At
231 the beginning of incubation, it was similar for both tissues. After 30 minutes there was a
232 significant increase in the amount of LDH, after which time it increased steadily. In both
233 tissues, the ileum showed higher values of LDH basolaterally. However, the
234 percentage of LDH in the basolateral side versus the total LDH (tissue plus basolateral)
235 was lower than 0.1%. We also compared the LDH leakage of ileum samples mounted
236 in the AtB to that of *ex vivo* free cultured ileum samples (of similar size). We found no
237 differences (nKatal: 1.40 ± 0.17 (basolateral AtB); 1.38 ± 0.29 (free)).

238 For our study it is essential for us to be able to work on the apical-to-basolateral effect
239 so, for this reason, the barrier function must be preserved. We initially used FITC-70
240 kDa to discount inadequate adhesion between biological tissue and the tube surface in
241 the AtB. **Figure 3a** shows that the amount of FITC-70 was approximately 0.1% in the
242 ileum samples and 0.5% in the colon samples, which suggests optimal adhesion.
243 Afterwards, we checked the barrier properties and compared them to those found when
244 a chambers system was used. Transepithelial electrical resistance (TEER)
245 measurements of various intestinal segments, with similar characteristics and assay
246 conditions, but mounted in an Ussing chamber apparatus provides information on the
247 integrity of the epithelia and their tightness. **Figure 3b** shows that the TEER varies
248 between the intestinal segments and that it decreased slightly only in duodenal

249 segments after a 60-minute incubation. Since TEER cannot be measured in the AtB
250 device, we measured the paracellular transport of Lucifer Yellow from apical to
251 basolateral compartments. **Figure 3c** shows that the amount of Lucifer yellow crossing
252 the ileum mucosa and submucosa is approximately 0.5% in both devices which had
253 equal surface areas (Ussing chamber: 0.5 cm² and AtB: 0.5024 cm²). The quantity of
254 Lucifer Yellow in the duodenum mounted in AtB was 0.21% ± 0.06, and in the
255 ascendant colon it was 1.62% ± 0.98.

256

257

258 Enteroendocrine function

259 The relative abundance of enteroendocrine cells in the various intestinal segments
260 depends on the species [26]. Here we show the differential basolateral secretion
261 pattern obtained in response to different apical stimulatory signals. **Figure 4a** shows
262 that non-stimulated secretion of PYY is higher in the duodenum than in the distal ileum.
263 Moreover, **figure 4b** shows that the distal ileum produces more GLP1 than the
264 proximal colon. Since several enteroendocrine cells are located in the epithelium of the
265 intestinal barrier, with the apical side in contact with the gastrointestinal duct, and the
266 basolateral side draining the internal body fluids, apical stimulation by some agents
267 should produce basolateral secretion of enterohormones (see **figure 4c**). Apically
268 applied IBMX produces a statistically significant stimulation of basolateral secretion of
269 active GLP1 at the ileum and only a slight stimulation in colonic segments.

270 To determine whether our setup could be used to screen enteroendocrine
271 secretagogues, we subjected our AtB setup to two treatments with potential bioactivity
272 for stimulating enterohormone secretion. **Figure 5a** shows that an animal extract
273 increased CCK and active ghrelin secretion at the duodenum and inhibited PYY
274 secretion. The same extract did not lead to any change in the secretion of active GLP-1

275 in the ileum or in the colon. A plant extract, which has been proved to be a satiating
276 agent in rats [27], produced a different profile of secretions. It increased colonic active
277 GLP1 secretion statistically. It showed a tendency to increase CCK and PYY in the
278 duodenum and had no effect on active GLP1 secretion in the ileum segment (**Figure**
279 **5b**).

280

281

282 **Discussion**

283 The study of enteroendocrine processes requires a sufficient amount of tissue to host
284 enough endocrine cells to enable hormone secretions to be measured. These
285 processes also need to be studied in different intestinal segments, since the
286 enteroendocrine cell populations are distributed differently throughout the
287 gastrointestinal tract [28]. Another key point is to preserve apical to basolateral
288 separation, which is usually found in vivo. What is more, many signals cannot cross the
289 intestinal barrier [24]. Ussing chambers are the gold standard procedure for this
290 purpose, but they are expensive and the number of chambers is limited [14].

291 Our Ap-to-Bas setup is an ex vivo system derived from the pig's intestinal wall, which
292 enables vectorial transepithelial processes to be assayed. This system has three main
293 advantages over the gold standard Ussing chambers method. It makes it possible to
294 work with more samples at the same time while maintaining transepithelial activity
295 affordably; it makes it possible to work with an animal model that is more similar to
296 human beings [20], and the size of the mucosal sample guarantees that the
297 enterohormones will be detected.

298 *Ex vivo* systems have limitations, such as the short-time viability of the tissue. We have
299 shown that when healthy intestines are mounted in the AtB system there is enough

300 time for the changes in enterohormone secretions to be measured. Westerhout and col
301 showed that LDH leakage of the intracellular enzyme into the basolateral media from
302 pig jejunal tissue segments mounted in their setup was $3.5 \pm 0.8\%$ [29]. The
303 percentage of leakage we found was lower than this, and the amount of LDH in the
304 basolateral media increased as it did in free cultured equivalent segments, which
305 suggests that the tissue was not damaged any further by being mounted in the AtB
306 setup.

307 Our system maintained the vectoriality required for processes that occur across a wall.
308 As we were working with glued surfaces, we discounted any problems in the adhesion
309 of the tissue by apically applying fluorescein (FITC)-labelled dextran (70 kDa), an agent
310 that is unable to cross the intestinal barrier [30] and is typically used to measure
311 gastrointestinal transit [31]. The absence of fluorescence from the basolateral side of
312 the AtB setup showed that the apical side had been optically insulated from the
313 basolateral side. Pierre et al. [21] also used this same approach to develop an ex vivo
314 intestinal segment culture (EVISC) model for studying the ex vivo effects of parenteral
315 nutrition on the susceptibility of the ileum to invasion by extra-intestinal pathogenic
316 *Escherichia coli* (ExPEC).

317 Evidence of the quality of the intestinal barrier was provided by various complementary
318 approaches. Lucifer Yellow unidirectional permeable paracellular marker [13] showed
319 that ileum segments were similarly permeable regardless of whether they were
320 mounted in AtB or the Ussing chamber. And the permeability of the ileum and colon
321 was similar. This similarity was also shown by Rozenhal working with Ussing chambers
322 and an area of exposure that was quite similar to our own (0.46 cm^2) [13]. The
323 percentage of LY leakage was also in the range that corresponded to an intact
324 intestinal barrier (0.5%) according to Westerhout, who was working with porcine
325 jejunal tissue and paracellular marker fluorescein isothiocyanate–dextran (FD4: MW 4
326 kDa) [29]. In fact, our values were slightly higher than those obtained by Westerhout et

327 al, but our compound was smaller (LY: MW 0.54 kDa) than theirs. They also worked
328 with different intestinal segments. Lennernäs [32] showed that MW correlated closely
329 with the permeability coefficients of hydrophilic drugs and that high permeability drugs
330 (BCS class I–II) showed a slightly higher permeability in the colon than the jejunum and
331 ileum when passive diffusion is the dominant transport mechanism.

332 To reinforce the integrity of the intestinal barrier and its standard state we compared
333 the TEER measures of various intestinal fragments. As we were unable to measure
334 TEER in our AtB setup, we worked with the same samples in the Ussing chamber
335 apparatus, which we have also used to measure human colonic samples for other
336 unpublished studies ($\Omega^* \text{ cm}^2$: 39.5 ± 2.2). Although the TEER measurements were
337 highly dependent on the assay condition and the best approach was to compare them
338 in the same study, the range of units obtained did not significantly differ from those
339 obtained by Westerhout et al. [29], who found a TEER of $58 \pm 7 \Omega \text{ cm}^2$, which remained
340 stable for 120 min when they used their device to work with porcine jejunal tissue. Also
341 working with Ussing chambers, Gleeson et al. [33] obtained a TEER of $37 \pm 9 \Omega \text{ cm}^2$
342 ($n=40$) in jejunal mucosae, which was within the acceptable range [30]. Jejunal TEER
343 gradually decreased over 120 min to 70–80% of the initial value. The lowest TEER
344 values we found were in colon segments, the result of different barrier properties
345 between intestinal segments. Permeability to small molecules and electrolytes was
346 lower in the duodenum, higher in the ileum and highly increased in the ascendant
347 colon. Hamilton et al. [34] and Moyano et al. [35] have shown that permeability to FITC
348 KD4 (and also various hydrophilic drugs [32]) follows a similar pattern in rat samples..

349 Our main reason for designing this setup was to be able to test the effects of
350 compounds on enterohormone secretion in a situation that more closely resembles the
351 physiological situation (i. e. several molecules in the gastrointestinal tube can only
352 stimulate enterohormone secretion by interaction with the apical side of these cells).
353 Very few studies have used ex-vivo approaches to determine vectorial enterohormone

354 secretion [14],[24]. Most studies use *ex-vivo* incubation of the intestine segment with
355 treatment in a multiwell plate [36], [37]. Pig intestine makes it possible to obtain
356 samples from various intestinal sections in sizes that are big enough to produce a
357 concentration of hormones secreted on the basolateral side that can be measured by
358 standard ELISA kits. Holst et al. described the enteroendocrine hormone abundance of
359 the various intestinal segments in different animal species [26]. The basolateral
360 secretion of PYY in duodenum and GLP1 in ileum was higher in our study than in their
361 description. We should point out that we are working with basolateral secretions,
362 although most of the available data has been published on the amount of hormone in
363 each intestinal segment, not secreted on the basolateral side [26,38,39]. Ripken and
364 Col studied the GLP1 and PYY released by pig intestinal sections, but they did not
365 compare them [16]. Similarly, Agersnap and col [40] assayed the relative presence of
366 CCK throughout the small intestine, and showed that it was more abundant in the first
367 20 centimetres after the pyloric sphincter, and Vitari and col [41] proved the presence
368 of ghrelin-producing cells in the duodenum of pigs. When we assayed an extract rich in
369 protein, we found a stimulation in CCK. Similarly, Sufian et al. compared this effect
370 between protein-derived extracts from different animals [42]. And, in fact, protein is a
371 very well defined secretagogue for CCK [43], [44]. We found that this protein-rich
372 extract had the specific effect of reducing PYY and stimulating acyl-ghrelin production,
373 although analysing this effect is beyond the scope of this manuscript.

374 To determine the possible physiological effects of this screening tool, we checked the
375 profile produced by an extract (GSPE [27]), which has been shown to have satiating
376 properties. The main components of this extract are flavanols and phenolic acids.
377 GSPE significantly increased GLP1 secretion, as previously shown *in vivo* [27] and *ex-*
378 *vivo*, by intestine tissue culture [45]. PYY, which significantly increased in our previous
379 *ex-vivo* approach [45], tended to increase too. In contrast, our different systems gave
380 different results for CCK. There may be several reasons for these differences: for

381 example, different responses between rat and pig, or the method for stimulating cells
382 (apically in the AtB vs around all the cells in an *ex-vivo* system).

383 In conclusion, our AtB setup is a tool for screening new agents that can act apically on
384 enteroendocrine cells in a physiological approach. This tool could be useful for
385 identifying new agents that can have an effect on the gut-brain axis.

386

387

388 **Acknowledgements**

389 We would like to thank the collaboration of the slaughterhouse in Alcover and Alcover
390 Town Council for providing all the samples needed for this study. This study was
391 funded by grant AGL2014-55347-R from the Spanish government. Iris Ginés and
392 Katherine Gil received a Marti-Franquès grant for PhD students from the Universitat
393 Rovira i Virgili. Paula Robles was funded by “Garantia Juvenil de Catalunya”.
394 Montserrat Pinent is a Serra Hünter fellow. We would like to thank Niurka Llopiz for her
395 technical support.

396

397 **Author Contributions Statement**

398 I.G., K. G-C. and P. R. have run all the laboratory tasks. M.P., A.A., X.T. and M.B.
399 designed the experiments and collected tissues. Ll. A. provided the tested samples. All
400 the authors discussed the results. I.G., M.P. and A.A. wrote the manuscript, which was
401 checked and discussed by all authors.

402

403 **Additional Information.**

404 **Competing financial interests**

405 The investigators have no conflict of interest relating to this study.

406

407 **References**

- 408 [1] F.M. Gribble, The gut endocrine system as a coordinator of postprandial nutrient
409 homoeostasis, *Proc. Nutr. Soc.* 71 (2012) 456–462.
- 410 [2] F.M. Gribble, F. Reimann, Signalling in the gut endocrine axis, *Physiol. Behav.*
411 176 (2017) 183–8. doi:10.1016/j.physbeh.2017.02.039.
- 412 [3] A.R. Gunawardene, B.M. Corfe, C.A. Staton, Classification and functions of
413 enteroendocrine cells of the lower gastrointestinal tract, *Int. J. Exp. Pathol.* 92
414 (2011) 219–231. doi:10.1111/j.1365-2613.2011.00767.x.
- 415 [4] G. de Lartigue, Role of the vagus nerve in the development and treatment of
416 diet-induced obesity., *J. Physiol.* 0 (2016) 1–25. doi:10.1113/JP271538.
- 417 [5] V. Dumoulin, F. Moro, A. Barcelo, T. Dakka, J.-C. Cuber, Peptide YY, Glucagon-
418 Like Peptide-1, and Neurotensin Responses to Luminal Factors in the Isolated
419 Vascularly Perfused Rat Ileum, *Endocrinology.* 139 (1998) 3780–3786.
420 doi:10.1210/endo.139.9.6202.
- 421 [6] G. Rindi, S. G. Grant, Y. Yiangou, M. A. Ghatei, S. R. Bloom, V. L. Batach, E.
422 Solcia, J.J. Polak; Development of neuroendocrine tumors in the gastrointestinal
423 tract of transgenic mice. Heterogeneity of hormone expression., *Am J Pathol.*
424 136 (1990) 1349–1363.
- 425 [7] D.J. Drucker, T. Jin, S.L. Asa, T.A. Young, P.L. Brubaker, Activation of
426 proglucagon gene transcription by protein kinase-A in a novel mouse
427 enteroendocrine cell line., *Mol. Endocrinol.* 8 (1994) 1646–1655.
428 doi:10.1210/mend.8.12.7535893.
- 429 [8] H. Iwakura, Y. Li, H. Ariyasu, H. Hosoda, N. Kanamoto, Establishment of a
430 Novel Ghrelin-Producing Cell Line, 151 (2016) 2940–2945.
431 doi:10.1210/en.2010-0090.
- 432 [9] T.-J. Zhao, I. Sakata, R.L. Li, G. Liang, J.A. Richardson, M.S. Brown, J.L.

- 433 Goldstein, J.M. Zigman, Ghrelin secretion stimulated by 1-adrenergic receptors
434 in cultured ghrelinoma cells and in fasted mice, *Proc. Natl. Acad. Sci.* 107 (2010)
435 15868–15873. doi:10.1073/pnas.1011116107.
- 436 [10] H.J. Kim, D.E. Ingber, Gut-on-a-Chip microenvironment induces human
437 intestinal cells to undergo villus differentiation., *Integr. Biol. (Camb).* 5 (2013)
438 1130–40. doi:10.1039/c3ib40126j.
- 439 [11] N. Van Der Wielen, J. Paul, S. Muckenschnabl, R. Pieters, H.F.J. Hendriks, R.F.
440 Witkamp, J. Meijerink, The Noncaloric Sweetener Rebaudioside A Stimulates
441 Glucagon-Like Peptide 1 Release and Increases Enteroendocrine Cell Numbers
442 in 2-Dimensional Mouse Organoids Derived from Different Locations of the
443 Intestine 1 – 4, *J. Nutr.* (2016) 1–7. doi:10.3945/jn.116.232678.1.
- 444 [12] M. Li, I.A.M. de Graaf, G.M.M. Groothuis, Precision-cut intestinal slices:
445 alternative model for drug transport, metabolism, and toxicology research.,
446 *Expert Opin. Drug Metab. Toxicol.* 12 (2016) 175–90.
447 doi:10.1517/17425255.2016.1125882.
- 448 [13] V. Rozehnal, D. Nakai, U. Hoepner, T. Fischer, E. Kamiyama, M. Takahashi, S.
449 Yasuda, J. Mueller, Human small intestinal and colonic tissue mounted in the
450 Ussing chamber as a tool for characterizing the intestinal absorption of drugs,
451 *Eur. J. Pharm. Sci.* 46 (2012) 367–373. doi:10.1016/j.ejps.2012.02.025.
- 452 [14] M.C.P. Geraedts, F.J. Troost, R.J. De Ridder, A.G.L. Bodelier, A.A.M. Masclee,
453 W.H.M. Saris, Validation of Ussing Chamber Technology to Study Satiety
454 Hormone Release From Human Duodenal Specimens, *Obesity.* 20 (2012) 678–
455 682. doi:10.1038/oby.2011.104.
- 456 [15] H. Yu, N.M. Hasan, J.G. In, M.K. Estes, O. Kovbasnjuk, N.C. Zachos, M.
457 Donowitz, The Contributions of Human Mini-Intestines to the Study of Intestinal
458 Physiology and Pathophysiology, *Annu. Rev. Physiol.* 79 (2017) 291–312.

- 459 doi:10.1146/annurev-physiol-021115-105211.
- 460 [16] D. Ripken, N. Van Der Wielen, H.M. Wortelboer, J. Meijerink, R.F. Witkamp,
461 H.F.J. Hendriks, Steviol glycoside rebaudioside A induces glucagon-like peptide-
462 1 and peptide YY release in a porcine ex vivo intestinal model, *J. Agric. Food*
463 *Chem.* 62 (2014) 8365–8370. doi:10.1021/jf501105w.
- 464 [17] M.C.P. Geraedts, F.J. Troost, W.H.M. Saris, Addition of sucralose enhances the
465 release of satiety hormones in combination with pea protein., *Mol. Nutr. Food*
466 *Res.* 56 (2012) 417–24. doi:10.1002/mnfr.201100297.
- 467 [18] J. Serrano, À. Casanova-Martí, I. Depoortere, M.T.M.T. Blay, X. Terra, M.
468 Pinent, A. Ardévol, Subchronic treatment with grape-seed phenolics inhibits
469 ghrelin production despite a short-term stimulation of ghrelin secretion produced
470 by bitter-sensing flavanols, *Mol. Nutr. Food Res.* 60 (2016) 2554–2564.
471 doi:10.1002/mnfr.201600242.
- 472 [19] B. Le Nevé, M. Foltz, H. Daniel, R. Gouka, The steroid glycoside H.g.-12 from
473 *Hoodia gordonii* activates the human bitter receptor TAS2R14 and induces CCK
474 release from HuTu-80 cells., *Am. J. Physiol. Gastrointest. Liver Physiol.* 299
475 (2010) G1368-75. doi:10.1152/ajpgi.00135.2010.
- 476 [20] E. Roura, S.-J. Koopmans, J.-P. Lallès, I. Le Huerou-Luron, N. de Jager, T.
477 Schuurman, D. Val-Laillet, Critical review evaluating the pig as a model for
478 human nutritional physiology, *Nutr. Res. Rev.* 29 (2016) 1–31.
479 doi:10.1017/S0954422416000020.
- 480 [21] J.F. Pierre, A.F. Heneghan, J.M. Meudt, M.P. Shea, C.G. Krueger, J.D. Reed,
481 K.A. Kudsk, D. Shanmuganayagam, Parenteral nutrition increases susceptibility
482 of ileum to invasion by e coli, *J. Surg. Res.* 183 (2013) 583–591.
483 doi:10.1016/j.jss.2013.01.054.
- 484 [22] E.M. Danielsen, G.H. Hansen, K. Rasmussen, L.-L. Niels-Christiansen,

- 485 Permeabilization of enterocytes induced by absorption of dietary fat., *Mol.*
486 *Membr. Biol.* 30 (2013) 261–72. doi:10.3109/09687688.2013.780642.
- 487 [23] D. Ripken, N. van der Wielen, H.M. Wortelboer, J. Meijerink, R.F. Witkamp,
488 H.F.J. Hendriks, Nutrient-induced glucagon like peptide-1 release is modulated
489 by serotonin., *J. Nutr. Biochem.* 32 (2016) 142–50.
490 doi:10.1016/j.jnutbio.2016.03.006.
- 491 [24] C.A. Brighton, J. Rievaj, R.E. Kuhre, L.L. Glass, K. Schoonjans, J.J. Holst, F.M.
492 Gribble, F. Reimann, Bile acids trigger GLP-1 release predominantly by
493 accessing basolaterally located G protein-coupled bile acid receptors,
494 *Endocrinology.* 156 (2015) 3961–3970. doi:10.1210/en.2015-1321.
- 495 [25] A. Fortuño-Mar, P. Pasquali, Cryobiopsy, Cryoanesthesia, and Cryoanalgesia,
496 in: *Cryosurgery*, Springer Berlin Heidelberg, Berlin, Heidelberg, 2015: pp. 85–91.
497 doi:10.1007/978-3-662-43939-5_7.
- 498 [26] N.J. Wewer Albrechtsen, R.E. Kuhre, S. Toräng, J.J. Holst, The intestinal
499 distribution pattern of appetite- and glucose regulatory peptides in mice, rats and
500 pigs., *BMC Res. Notes.* 9 (2016) 60. doi:10.1186/s13104-016-1872-2.
- 501 [27] J. Serrano, À. Casanova-Martí, K. Gil-Cardoso, M.T. Blay, X. Terra, M. Pinent,
502 A. Ardévol, Acutely administered grape-seed proanthocyanidin extract acts as a
503 satiating agent., *Food Funct.* 7 (2016) 483–90. doi:10.1039/c5fo00892a.
- 504 [28] R.E. Steinert, C. Beglinger, Nutrient sensing in the gut: Interactions between
505 chemosensory cells, visceral afferents and the secretion of satiation peptides,
506 *Physiol. Behav.* 105 (2011) 62–70. doi:10.1016/j.physbeh.2011.02.039.
- 507 [29] J. Westerhout, E. Van De Steeg, D. Grossouw, E.E. Zeijdner, C.A.M. Krul, M.
508 Verwei, H.M. Wortelboer, A new approach to predict human intestinal absorption
509 using porcine intestinal tissue and biorelevant matrices, *Eur. J. Pharm. Sci.* 63
510 (2014) 167–177. doi:10.1016/j.ejps.2014.07.003.

- 511 [30] J. Serrano, À. Casanova-Martí, M. Blay, X. Terra, A. Ardévol, M. Pinent, Defining
512 Conditions for Optimal Inhibition of Food Intake in Rats by a Grape-Seed
513 Derived Proanthocyanidin Extract., *Nutrients*. 8 (2016) 652.
514 doi:10.3390/nu8100652.
- 515 [31] J. Schmidt, B. Stoffels, A. Nazir, D. L. Dehaven-Hudkins, A. J. Bauer,
516 Alvimopan and COX-2 inhibition reverse opioid and inflammatory components of
517 postoperative ileus, *Neurogastroenterol. Motil.* 20 (2008) 689–699.
518 doi:10.1111/j.1365-2982.2007.01078.x.
- 519 [32] H. Lennernäs, Animal data: The contributions of the Ussing Chamber and
520 perfusion systems to predicting human oral drug delivery in vivo, *Adv. Drug*
521 *Deliv. Rev.* 59 (2007) 1103–1120. doi:10.1016/j.addr.2007.06.016.
- 522 [33] J.P. Gleeson, D.J. Brayden, S.M. Ryan, Evaluation of PepT1 transport of food-
523 derived antihypertensive peptides, Ile-Pro-Pro and Leu-Lys-Pro using in vitro , ex
524 vivo and in vivo transport models, *Eur. J. Pharm. Biopharm.* 115 (2017) 276–
525 284. doi:10.1016/j.ejpb.2017.03.007.
- 526 [34] H.E. Hamilton, M K; Boudry, G; Lemay, D G; Raybould, Changes in intestinal
527 barrier function and gut microbiota in high-fat diet-fed rats are dynamic and
528 region dependent, *Am J Physiol Gastrointest Liver Physiol.* 308 (2015) G840-51.
529 doi:10.1152/ajpgi.00029.2015.
- 530 [35] V. Moyano-Porcile, L. Olavarría-Ramírez, C. González-Arancibia, J.A. Bravo, M.
531 Julio-Pieper, Short-term effects of Poly(I:C) on gut permeability, *Pharmacol. Res.*
532 101 (2015) 130–136. doi:10.1016/j.phrs.2015.06.016.
- 533 [36] T. Voortman, H.F.J. Hendriks, R.F. Witkamp, H.M. Wortelboer, Effects of long-
534 and short-chain fatty acids on the release of gastrointestinal hormones using an
535 ex vivo porcine intestinal tissue model, *J. Agric. Food Chem.* 60 (2012) 9035–
536 9042. doi:10.1021/jf2045697.

- 537 [37] R. Pais, J. Rievaj, P. Larraufie, F. Gribble, F. Reimann, Angiotensin II Type 1
538 Receptor-Dependent GLP-1 and PYY Secretion in Mice and Humans,
539 Endocrinology. 157 (2016) 3821–3831. doi:10.1210/en.2016-1384.
- 540 [38] R.E. Kuhre, N.W. Albrechtsen, J.A. Windelov, B. Svendsen, B. Hartmann, J.J.
541 Holst, GLP-1 amidation efficiency along the length of the intestine in mice, rats
542 and pigs and in GLP-1 secreting cell lines, Peptides. 55 (2014) 52–57.
543 doi:10.1016/j.peptides.2014.01.020.
- 544 [39] H.-J. Cho, S. Kosari, B. Hunne, B. Callaghan, L.R. Rivera, D.M. Bravo, J.B.
545 Furness, Differences in hormone localisation patterns of K and L type
546 enteroendocrine cells in the mouse and pig small intestine and colon., Cell
547 Tissue Res. 359 (2015) 693–8. doi:10.1007/s00441-014-2033-3.
- 548 [40] M. Agersnap, J.F. Rehfeld, Nonsulfated cholecystokinins in the small intestine of
549 pigs and rats., Peptides. 71 (2015) 121–7. doi:10.1016/j.peptides.2015.07.010.
- 550 [41] F. Vitari, A. Di Giancamillo, D. Deponti, V. Carollo, C. Domeneghini, Distribution
551 of ghrelin-producing cells in the gastrointestinal tract of pigs at different ages.,
552 Vet. Res. Commun. 36 (2012) 71–80. doi:10.1007/s11259-012-9517-y.
- 553 [42] M. SUFIAN, T. HIRA, K. MIYASHITA, T. NISHI, K. ASANO, H. HARA, Pork
554 Peptone Stimulates Cholecystokinin Secretion from Enteroendocrine Cells and
555 Suppresses Appetite in Rats, Biosci. Biotechnol. Biochem. 70 (2006) 1869–
556 1874. doi:10.1271/bbb.60046.
- 557 [43] M.C.P. Geraedts, F.J. Troost, M.A.J.G. Fischer, L. Edens, W.H.M. Saris, Direct
558 induction of CCK and GLP-1 release from murine endocrine cells by intact
559 dietary proteins, Mol. Nutr. Food Res. (2010) n/a-n/a.
560 doi:10.1002/mnfr.201000142.
- 561 [44] M.C.P. Geraedts, F.J. Troost, W.H.M. Saris, Gastrointestinal targets to modulate
562 satiety and food intake, Obes. Rev. (2010) no-no. doi:10.1111/j.1467-

563 789X.2010.00788.x.

564 [45] À. Casanova-Martí, J. Serrano, M.T. Blay, X. Terra, A. Ardévol, M. Pinent, Acute
565 selective bioactivity of grape seed proanthocyanidins on enteroendocrine
566 secretions in the gastrointestinal tract., Food Nutr. Res. 61 (2017) 1321347.
567 doi:10.1080/16546628.2017.1321347.

568

569 **Figure captions.**

570 **Figure 1. Representative pictures describing the building of the AtB**

571 a) After the outer muscle layers had been removed, the intestinal tube was cut open
572 longitudinally. Circles of tissue with a diameter of 14 mm (approximately 1.54 cm²)
573 were punched out using a biopsy punch; b), the intestine was placed in a cell culture
574 insert with no bottom membrane; c) Finally, the whole insert was placed in a well of a
575 12-well plate prefilled with 1 ml of KRB buffer (with D-Glucose 10 mM). Apically, the
576 tube was filled with 400 µl of KRB buffer (with D-Mannitol 10 mM).

577

578 **Figure 2** Haematoxilin-eosin staining of transversal thin sections from a pig's A)
579 duodenum, B) ileum and C) colon mucosa (original magnification, ×6). The images
580 show mucosa and submucosa of each section of intestine. The scale bar indicates 0.2
581 mm.

582 **Figure 3a.** Percentage of FITC dextran 70 kDa in the basolateral side in ileum and
583 colon AtB. FICT 70 kDa was added to the apical side of the AtB setup and, after 60
584 minutes of incubation at 37 °C, the percentage of FITC on the basolateral side was
585 measured. Values are the mean± SEM.

586

587

588 **Figure 3b.** Transepithelial electrical resistance (TEER) of different intestinal segments
589 during the incubation period.

590 Barrier integrity measured as transepithelial electrical resistance (TEER) in $\Omega \cdot \text{cm}^2$ at
591 the start of incubation (black columns) and after 60 minutes of incubation at 37 °C
592 (white columns). Tissues were mounted in Ussing chambers and were incubated at 37
593 °C for 60 minutes. Values are means \pm SEM. * $P < 0.05$ when the incubation start time
594 of each tissue is compared with 60 minutes (T-Student). One-way anova $P < 0.05$ was
595 used to compare differences between the start time of each tissue; differences,
596 obtained by T3-Dunnnett post-hoc test, were defined by different letters.

597

598 **Figure 3c.** Percentage of Lucifer Yellow (LY) crossing the ileum wall on the basolateral
599 sides of Ussing chambers and AtB.

600 LY was added to the apical side of both approaches and, after 60 minutes of
601 incubation at 37 °C, the percentage of LY on the basolateral side was measured.
602 Values are the mean \pm SEM.

603

604 **Figure 4a:** Basolaterally secreted PYY under unstimulated conditions at different
605 anatomical locations.

606 Different Ap-to-Bas setups were mounted for each intestinal porcine duodenum (black
607 column) and ileum (grey column) (n=8 for each section). After 60 minutes in the C-
608 buffer, basolateral media were collected and hormone levels of peptide YY (PYY) were
609 measured. Values are percentage \pm SEM. * $p < 0.05$ vs duodenum.

610 **Figure 4b:** Ileum and colon relative basal secretion into basolateral media of GLP1.

611 Different Ap-to-Bas setups were mounted for each intestinal porcine ileum (black
612 columns) and colon (squared columns) (n=5 for each section). After 60 minutes in the
613 C-buffer, basolateral media were collected and hormone levels of total and active
614 GLP1, were measured. Values are percentage \pm SEM. * p < 0.05 vs ileum.

615 **Figure 4c:** Sensitivity of ileum and colon segments to apical IBMX stimulation of active-
616 GLP-1 secretion

617 Different Ap-to-Bas setups were mounted for each intestinal porcine ileum and colon
618 (n=5 for each section). IBMX (20 μ M) was apically applied (white columns). Black
619 columns refer to unstimulated controls. At the end of the treatment (60 minutes),
620 basolateral media were collected and active GLP1 was measured. Values are
621 percentage \pm SEM. * p < 0.05 compared to negative (vehicle treated) control (C-)

622 **Figure 5a.** Basolateral enteroendocrine secretions after apical stimulation with
623 homogenates of animal origin in AtB setups

624 Different Ap-to-Bas setups were mounted for each intestinal porcine duodenum (black
625 columns), ileum (grey column) and colon (striped column) (n=8 for each section).
626 Animal extracts (10 mg protein/ mL) were apically applied. At the end of the treatment
627 (duodenum: 90 min; others: 60 min) basolateral media were collected and hormone
628 levels of cholecystokinin (CCK), peptide YY (PYY), active ghrelin and active glucagon(-
629 like) peptide 1 (GLP-1) were measured. Values are percentage \pm SEM. * p < 0.05
630 compared to negative (vehicle treated) control (C-)

631 **Figure 5b.** Basolateral enteroendocrine secretions after apical stimulation with plant
632 extract in AtB setups.

633 Different Ap-to-Bas setups were mounted on each intestinal porcine duodenum (black
634 columns), ileum (grey column) and colon (striped column) (n=8 replicates). Plant

635 extracts (100 mg extract/ mL) were applied apically. At the end of the treatment,
636 basolateral media were removed and hormone levels of cholecystokinin (CCK), peptide
637 YY (PYY) and active glucagon such as peptide 1 (GLP-1) were measured. Values are
638 percentage \pm SEM. * $p < 0.05$, # $p < 0.1$ compared to the negative control (C-).

639

640

Table 1. LDH leakage on the basolateral side of the AtB throughout the incubation

	0 minutes		30 minutes		60 minutes	
	nKatal	SEM	nKatal	SEM	nKatal	SEM
Ileum	0.46^A	0.04	1.40^B	0.17	1.92^B	0.18
Colon	0.31^A	0.05	0.74^B	0.07	0.99^B	0.13

LDH in the basolateral media was measured at different times. Values are the mean \pm SEM. Statistical differences were calculated using one-way ANOVA followed by a T3-Dunnnett post-hoc. Different superscripts mean statistical differences between times. A p value < 0.05 was considered to be statistically significant.

641

Figure 1a:

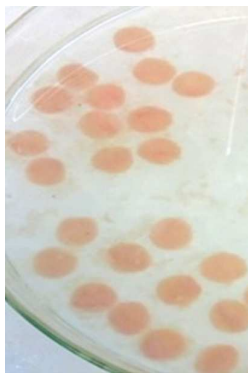
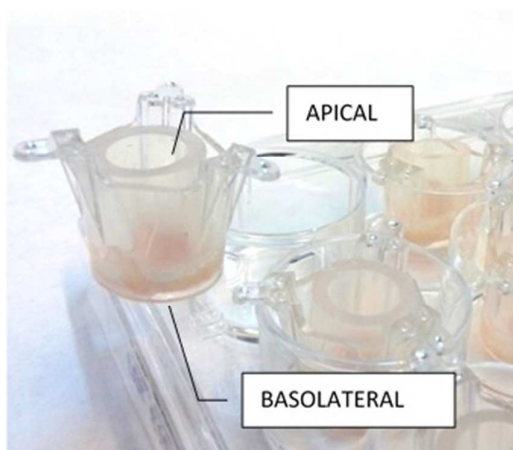


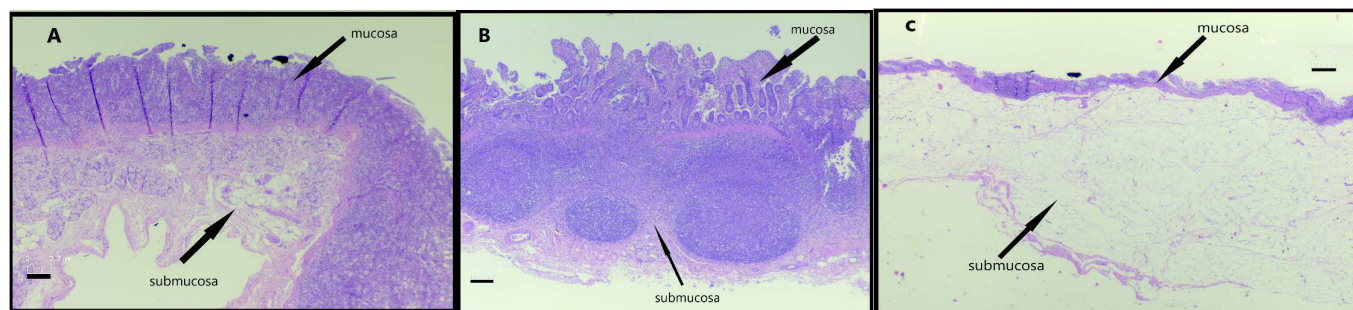
Figure 1b:



Figure 1c:



643 Figure 2:



644

645

646

647

Figure 3a:

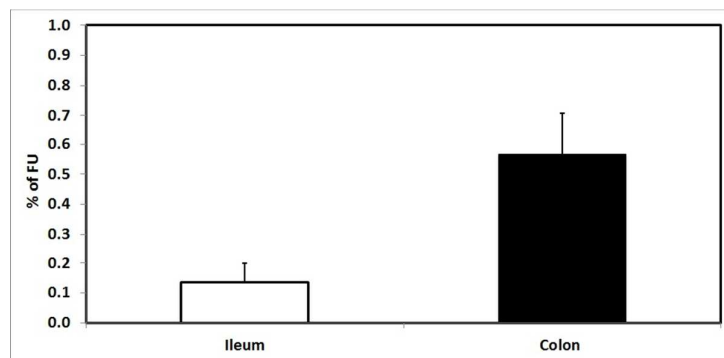


Figure 3b:

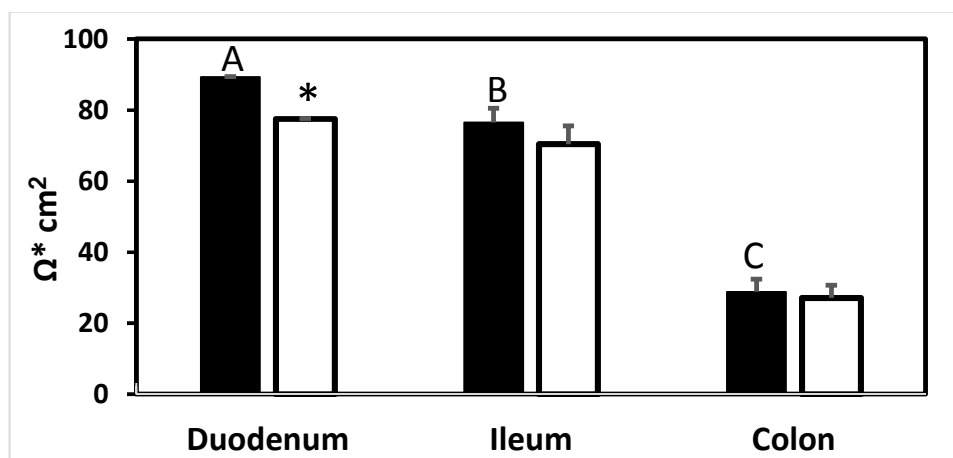


Figure 3c:

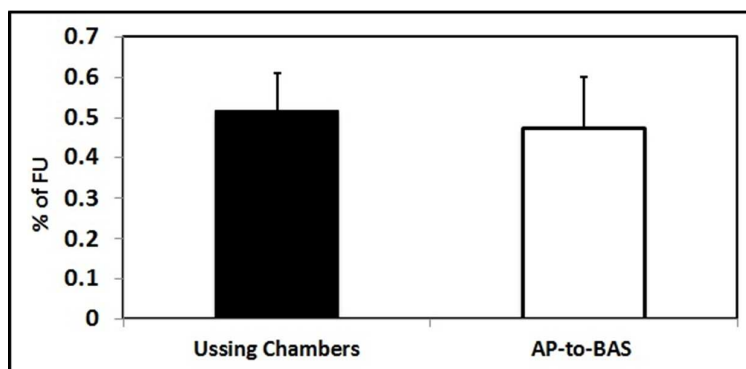


Figure 4a:

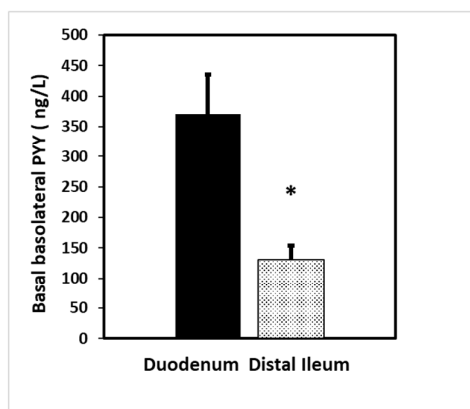


Figure 4b:

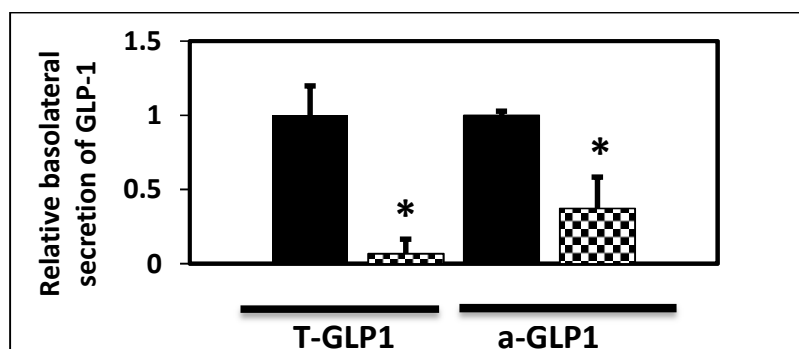


Figure 4c:

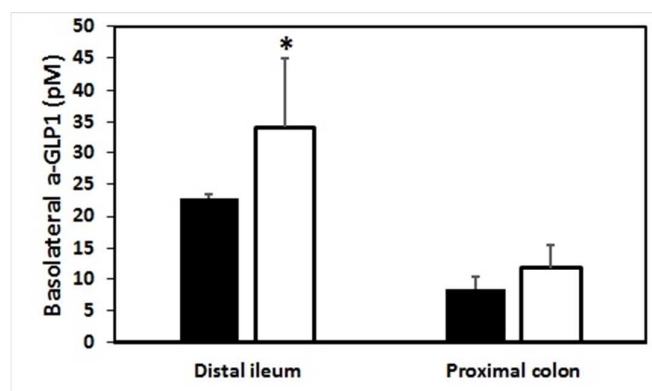


Figure 5a:

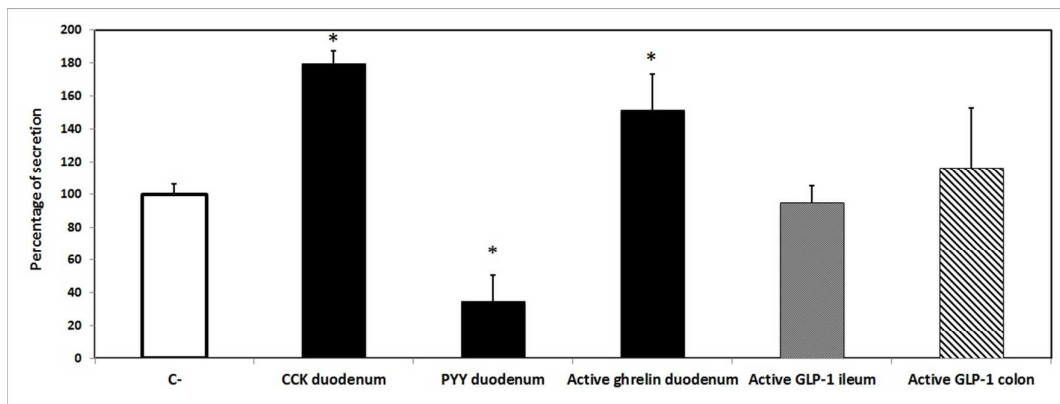
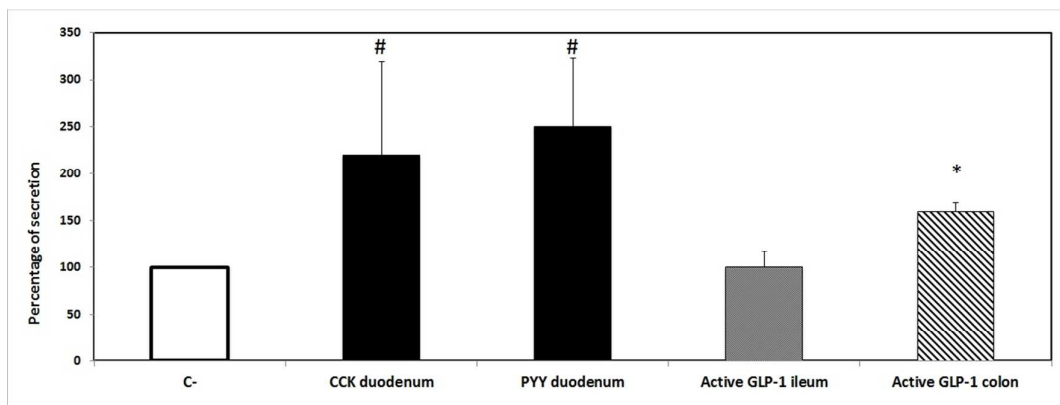


Figure 5b:

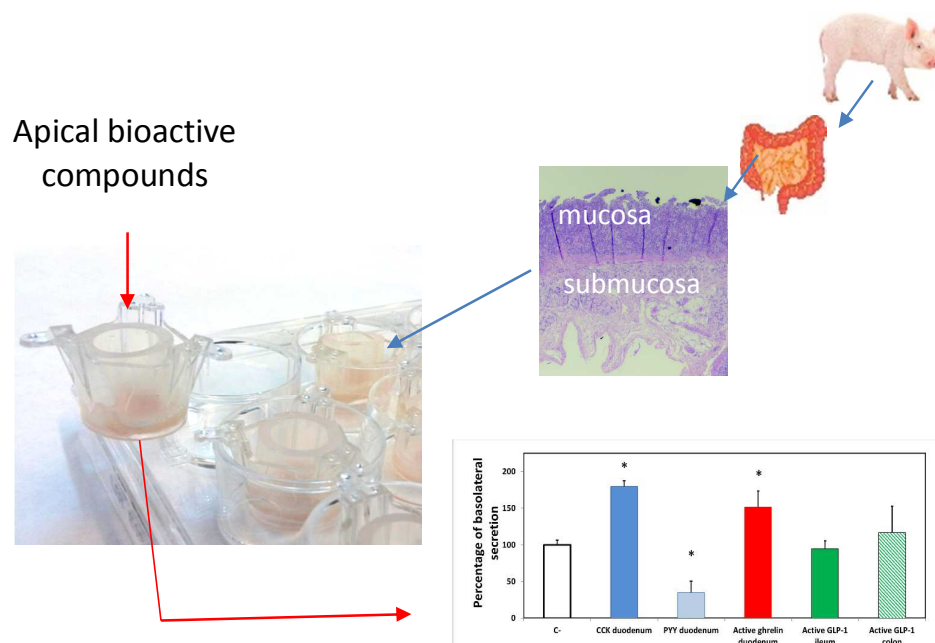


648

649

TOC

650



Apical bioactive compounds

